Magnesium diethynylporphyrin derivatives with strong near-infrared absorption for solution-process bulk heterojunction organic solar cells

Keisuke Ogumi[a,b], Takafumi Nakagawa[c], Masahiro Nakano[d] and Yutaka Matsuo*[b,c,e]

[a] *Tokyo Metropolitan Industrial Technology Research Institute, 2-4-10 Aomi, Koto-ku, Tokyo 135-0064, Japan*

[b] *Department of Materials Science and Engineering, School of Engineering, Nagoya University, Furo-cho, Chikusa-ku, Nagoya 464-8603, Japan*

[c] *Department of Mechanical Engineering, School of Engineering, The University of Tokyo, 7-3-1 Hongo, Bunkyo-ku, Tokyo 113-8656, Japan*

[d] *Graduate School of Natural Science and Technology, Kanazawa University, Kakuma-machi, Kanazawa 920-1192, Japan*

[e] *Institutes of Innovation for Future Society, Nagoya University, Furo-cho, Chikusa-ku, Nagoya 464-8603, Japan*

Received date (to be automatically inserted after your manuscript is submitted)
Accepted date (to be automatically inserted after your manuscript is accepted

ABSTRACT: Magnesium diethynylporphyrin derivatives with strong near-infrared absorption were obtained. Those derivatives have electron rich units directly introduced to the porphyrin core. The electron rich units caused strong absorption on the near-infrared region because of an intramolecular charge transfer. Theoretical calculation also proved those derivatives showed large oscillator strength at the Q band. As a donor material, such large absorption coefficient in the range of long wavelength region is a desirable characteristic for organic solar cells. Organic photovoltaic devices using those diethynylporphyrin derivatives gave a PCE of 2.91% in the best condition.

KEYWORDS: porphyrin, strong absorption, intramolecular charge transfer, organic solar cells

*Correspondence to: Department of Materials Science and Engineering, School of Engineering, Nagoya University, Furo-cho, Chikusa-ku, Nagoya 464-8603, Japan
E-mail: yutaka.matsuo@chem.material.nagoya-u.ac.jp

INTRODUCTION

Small molecule organic solar cells (OSCs) have many advantages in fabrication process of OSCs. For example, small molecule donors are suitable for solution-process fabrication of OSCs because of good solubility. Furthermore, as they could be easily synthesized and purified, the device performance with them shows superior reproducibility. In recent years, many efforts on small molecule OCSs have been performed [1-7]. Porphyrin derivatives are well known as useful small molecule donors due to their high stability, high light absorption coefficient, and easiness of chemical modification. Although there are porphyrin derivatives coordinating with various metals, mostly zinc porphyrin complexes are employed for OSCs application [8-14]. We have synthesized magnesium porphyrin derivatives, because a magnesium atom favorably interacts with coordinating solvents and it increases solubility [15-18]. We also have revealed that magnesium porphyrin derivatives have long exciton lifetime compared with zinc analogues [19]. We consider these characteristics of magnesium porphyrin will improve performance of OSCs devices.

As a recent trend, porphyrin derivatives bearing a light absorption unit such as a diketopyrrolopyrrole (DPP) unit were often reported [20-26]. In those porphyrin derivatives, ethynyl bridges were used as linkers between the DPP units and the porphyrin core with its *meso*-position for the expansion of π-conjugated systems and the flatness of molecular structures. We have so far designed and synthesized magnesium tetraethynylporphyrin-DPP derivatives with four ethynyl linkers [27-29]. The tetraethynyl structure consolidates the coordination between the magnesium atom and the nitrogen atoms of the porphyrin core. This structure also causes long wavelength light absorption up to the near infrared region due to the expansion of π-conjugated systems throughout the molecule. Although magnesium tetraethynyl porphyrin derivatives exhibited usefulness as a small molecule donor for OSCs, low solubility because of the strong intermolecular π-π stacking was found to be limited. Generally, to improve the solubility, the long alkyl chain groups are introduced to the porphyrin core. However, the bulky chain units seem to have bad influence on morphology and charge carrier mobility of the active layers since these units hinder the intermolecular interaction.

To solve that solubility problem, we previously focused on an asymmetric porphyrin structure and thought the asymmetric structure might properly disordered the intermolecular packing. Thus, we synthesized magnesium tetraethynyl asymmetric porphyrin derivatives with two DPP units and two different aryl units. These asymmetric porphyrins in fact showed remarkable solubility than symmetric porphyrin analogues [30]. However, those asymmetric porphyrins demanded multistep Sonogashira cross coupling reactions to introduce the differ aryl units and it was difficult to prepare in large quantities.

Herein, we altered the tetraethynyl structure to a diethynyl structure to decrease the symmetry for easy synthesis, where we removed two ethynyl bridges from our pervious compounds (Figure 1). These diethynylporphyrin derivatives have electron rich units directly connected with the porphyrin core to construct donor-acceptor conjugates to have long-wavelength and strong light absorption. Electron rich units were expected to have an orthogonal structure to the porphyrin core and they consequently serve to disorder the intermolecular packing for good solubility without bulky alkyl chain units. Furthermore, we found with this structure that coordination between the magnesium atom and the porphyrin is strong enough. We also revealed the electron rich units influenced on photophysical property through the intramolecular charge transfer. This is the first report to synthesize magnesium diethynylporphyrin derivatives for OSCs application.

Please embed Fig 1. here.

EXPERIMENTAL

General

All reactions dealing with air- or moisture-sensitive compounds were carried out in a dry reaction vessel under nitrogen or argon. All reactions were monitored by thin layer chromatography (TLC, eluent, CH_2Cl_2). NMR spectra were measured on a JEOL ECA-600 spectrometer reported in parts per million from tetramethylsilane.High-resolution mass spectra were acquired by MALDI using a time-of-flight mass analyzer on Bruker Ultra exTOF/TOF spectrometer. UV–vis–NIR absorption spectra were recorded on JASCO V-670 spectrometer. Cyclic voltammetry (CV) and DPV were performed using a HOKUTO DENKO HZ-5000 voltammetric analyzer. All CV measurements were carried out in a one-compartment cell under argon gas, equipped with a glassy-carbon working electrode, a platinum wire counter electrode, and an Ag/Ag+ reference electrode. The solvent with supporting electrolyte was a 0.1 mol/L dichloromethane solution of tetrabutylammonium hexafluorophosphate ($TBAPF_6$). Ionization potential was measured by a RIKEN KEIKI AC-3 PYS in air. Current–voltage (J–V) characteristics were measured using a source meter (Keithley 2400) under 1 Sun AM 1.5G simulated sunlight irradiation (100 mW/cm^2) from a solar simulator (EMS-35AAA, Ushio Spax Inc.), which was calibrated using a silicon diode (BSe520BK, Bunkoukeiki).

Materials

Materials were purchased from Tokyo Kasei (TCI) Co., SigmaAldrich Inc., and other commercial suppliers and used after appropriate purification. Anhydrous solvents (stabilizer-free) were purchased from WAKO Pure Chemical.

Synthesis

Synthesis of [5,15-Bis(2,5-bis-(2-ethyl-hexyl)-3,6-di-thienyl-2-yl-2,5-dihydro-pyrrolo[3,4-c] pyrrole-1,4-dione-5'-yl-ethynyl)-10,20-bis(2,2'-dithienyl)-porphyrionate]magnesium(II) (2a)

A solution of precursor (35.0 mg, 0.034 mmol) in THF (4.1 mL) was added tetrabutylammonium fluoride (TBAF 1 mol/L in THF 0.10 mL, 0.10 mmol). After stirring for 30 min, THF (9.8 mL), NEt_3 (3.8 mL), DPP bromide (41.4 mg, 0.069 mmol), $Pd_2(dba)_3$ (1.57 mg, 1.72 μmol), PPh_3 (9.00 mg, 0.034 mmol), and CuI (0.33 mg, 1.72 μmol) were added. After heating at 85 °C for 1 h, the mixture was purified with silica gel column by using $CHCl_3$/THF (100/1) as eluent, and then purified with preparative GPC (JAIGEL-1H and JAIGEL-2H column, $CHCl_3$/THF=100/1). The solvent was removed under reduced pressure to give the desired product as blackish dark purple powder (24.8 mg, 42% yield). ^{1}H NMR (600 MHz; THF-d_8; Me_4Si): δ_H, ppm 0.79_0.93 (24H, m, CH_3), 1.19_1.45 (32H, m, CH_2), 1.85_2.01 (4H, br, CH), 4.00_4.15 (8H, m, CH_2), 7.05_7.07 (2H, m), 7.23 (2H, t, J = 4.2 Hz), 7.38 (2H, m), 7.41 (2H, m), 7.60 (2H, d, J = 3.6 Hz), 7.72_7.73 (2H, m), 7.77 (2H, d, J = 4.8 Hz), 7.84 (2H, d, J = 4.2 Hz), 9.05_9.08 (6H, m), 9.21 (2H, d, J = 3.6 Hz), 9.50 (4H, d, J = 4.2 Hz). ^{13}C NMR (150 MHz; THF-d_8; Me_4Si): δ_C, ppm 9.34, 9.41, 13.01, 13.16, 17.47, 22.60, 22.67, 22.86, 23.00, 27.82, 28.00, 29.66, 29.69, 29.79, 29.81, 38.81, 39.08 (two peaks, overlapped), 44.94, 45.05, 89.05, 101.06, 102.27, 107.42, 108.20, 114.80, 112.28, 123.31, 124.26, 127.49, 127.75, 128.55, 129.51, 130.01, 130.30, 130.72, 131.94, 132.08, 133.81, 135.32, 135.46, 136.82, 138.16, 139.59, 139.72, 142.26, 149.83, 151.00, 160.60, 160.67. APCI-HRMS (+) (m/z): calcd for $C_{98}H_{92}MgN_8O_4S_8$ (M+): 1724.4858, found 1724.4852.

Synthesis of [5,15-Bis(2,5-bis-(2-ethyl-hexyl)-3,6-di-thienyl-2-yl-2,5-dihydro-pyrrolo[3,4-c] pyrrole-1,4-dione-5'-yl-ethynyl)-10,20-bis(N-ethylcarbazole)-porphyrionate]magnesium(II) (2b)

A solution of precursor (91.0 mg, 0.084 mmol) in THF (10.1 mL) was added tetrabutylammonium fluoride (TBAF 1 mol/L in THF 0.25 mL, 0.25 mmol). After stirring for 30 min, THF (24.2 mL), NEt3 (9.2 mL), DPP bromide (101.9 mg, 0.169 mmol), $Pd_2(dba)_3$ (3.86 mg, 4.22 μmol), PPh_3 (22.1 mg, 0.068 mmol), and CuI (0.80 mg, 4.22 μmol) were added. After heating at 85 °C for 1 h, the mixture was purified with silica gel column by using $CHCl_3$/THF (100/1) as eluent, and then purified with preparative GPC (JAIGEL-1H and JAIGEL-2H column, $CHCl_3$/THF=100/1). The solvent was removed under reduced pressure to give the desired product as blackish dark purple powder (79.0 mg, 53% yield). ^{1}H NMR (600 MHz; THF-d_8; Me_4Si): δ_H, ppm 0.69_0.82 (24H, m, CH_3), 0.87 (6H, t, J = 7.2 Hz, CH_3), 1.17_1.40 (32H, m, CH_2), 1.82_1.96 (4H, br, CH), 4.01_4.10 (8H, m, CH_2), 4.61 (4H, q, J = 6.6 Hz, CH_2), 7.13 (2H, t, J = 5.4 Hz), 7.17 (2H, br), 7.43 (2H, t, J = 7.8 Hz), 7.56 (2H, d, J = 9.0 Hz), 7.66 (2H, d, J = 4.8 Hz), 7.71 (2H, br), 7.76 (2H, d, J = 8.4 Hz), 8.13 (2H, d, J = 7.8 Hz), 8.19 (2H, d, J = 8.4 Hz), 8.73 (4H, d, J = 4.2 Hz, Porphyrin), 8.83 (2H, s), 8.93 (2H, br), 9.08 (2H, s), 9.43 (4H, d, J = 3.6 Hz Porphyrin). ^{13}C NMR (150 MHz; THF-d_8; Me_4Si): δ_C, ppm 9.47, 9.54, 9.56, 12.91, 12.94, 13.00, 22.54, 22.59, 23.17, 23.29, 24.44, 28.01, 28.13, 29.22, 29.92, 29.95, 30.02, 30.05, 37.21, 38.96, 39.19, 45.19, 45.29, 88.88, 100.08, 103.22, 105.74, 107.75, 108.27, 108.32, 118.26, 120.11, 121.45, 122.96, 125.38, 125.51, 126.12, 127.65, 129.19, 129.37, 129.68, 130.00, 130.25, 131.57, 132.44, 132.52,133.44, 134.93, 135.40, 138.48, 139.34, 139.45, 140.83, 150.26, 150.80, 160.77. APCI-HRMS (+) (m/z): calcd for C110H106MgN10O4S4 (M+): 1782.7132, found 1782.7128.

Theoretical calculation

The Gaussian 09 package was used as a computational method. To calculate of the optimized structures of porphyrin dimers, we employed the polarized split-valence 6-31G(d) basis set and B3LYP function. In the calculation of the intermolecular interaction energies, the route section was # B97D3 /6-31G(d) counterpoise=2. Furthermore, in the estimate of energies of the optimized monomer, the route section was # sp B97D3 /6-31G(d).

Fabrication and elaluation of OSC devices

The patterned ITO substrates were cleaned by sonicating for 15 min in deionized water containing 5% surfactant (Semi Clean M-LO), distilled water, acetone, and isopropyl alcohol. The substrates were then dried using a N_2 gun and subjected to 15 min UV/O_3 treatment. Next, a filtered PEDOT:PSS (Clevios PVP Al4083) solution was deposited on the substrate via spin-coating (3000 rpm for 30 s) followed by thermal annealing in air for 10 min at 120 °C. These devices were carried to the glovebox and the active layer was deposited in the N_2 atmosphere. A 30 mg/mL solution of porphyrin derivatives and $PC_{61}BM$ in PhCl with 1% pyridine (vol %) was prepared with a 1:1.5 w/w donor/acceptor ratio. The solution was allowed to keep at 80 °C for 1 h in a nitrogen atmosphere. The films were prepared by spin-coating at 1000 rpm for 30 s. The substrates were transferred into a vacuum chamber. LiF and Al were deposited with thickness of 0.6 nm and 80.0 nm, respectively. Theactive area (0.04 cm^2) was defined by the geometric overlap between Aland ITO. The thickness of the thin films was measured with a DekTak 150 (Veeco Instruments Inc.).

RESULTS AND DISCUSSION

Scheme 1 shows the synthetic routes of magnesium diethynylporphyrin derivatives **2a** and **2b**. Although previous asymmetric porphyrin derivatives needed 6 steps from the formation of the porphyrin core, diethynylporphyrin derivatives were obtained through 4 steps because the formation of the porphyrin core and the introduction of electron rich units occurred at the same time. Therefore, diethynyl porphyrin derivatives were easily synthesized by using the corresponding aldehyde materials with electron rich units. We employed dithienyl and carbazole groups as the electron rich units because those aldehyde precursors were commercially available. Compound **2a** and **2b** shows good solubility towards several organic solvents, e.g. THF, chloroform, dichloromethane. Those compounds were black solid and dark red color in the organic solution (Scheme 1).

Please embed Scheme 1. here.

As a central metal, zinc atom was mostly employed in diethynylporphyrin structure and magnesium analogue has not yet been obtained. The main reason for that is the difference of the size of the central metal ions. The magnesium atom, which is smaller than zinc atom, could be off from the porphyrin core at high temperature. This desorption of the central metal is caused by protonation at the nitrogen atoms. Among porphyrin derivatives, magnesium porphyrins with the tetraethynyl porphyrin structure can decrease the electronegativity of the nitrogen atoms to prevent that undesired metal ion desorption. While diethynylporphyrin structure was employed in this research, the desorption of magnesium atom was not observed during heating the reaction. It was explained that the electronegativities of nitrogen atoms were depended on the DPP units and those could sufficiently hold the magnesium atom in even diethynylporphyrin structure. This expectation was supported by the theoretical calculation.

The electron rich units also had merits for photophysical property. Firstly, it was concerned that the convert from tetraethynyl to diethynyl structure caused the disunion of π-conjugated systems and decreased the absorption efficiency among long wavelength region owing to the expansion of energy band gap. Figure 2 showed UV-vis spectra of compound **2a**, **2b** and symmetric tetraethynylporphyrin derivative **3** as a reference. The near-infrared absorptions were Q band peaks which were attributed to the porphyrin core. Focusing on those peaks, the positions of peak top were not significantly different for all compounds. This result revealed that compound **2a** and **2b** having the electron rich units did not cause the disunion of π-conjugated systems. Furthermore, compound **2b** with the carbazole units had a lager and wider wavelength absorption than that of **3**. Generally, in porphyrin derivatives, a maximum absorption is a Soret band peak. However, compound **2b** exhibited a maximum peak in the Q band area. This observation was derived from the strong intramolecular charge transfer by the carbazole units and suggested that compound **2b** had good photophysical property as a donor material.

Please embed Fig 2. here.

Electrochemical properties of compound **2a**, **2b** and **3** were shown in Table 1. In the THF solution state, compound **2b** had the narrowest HOMO/LUMO energy bang gap. This explained that the electron rich units directly connecting to the porphyrin core also affected energy levels as with the DPP units. In the thin film state, the HOMO levels were determined by photoemission yield spectroscopy and the band gaps were measured by UV-vis spectroscopy and the LUMO levels subsequently were estimated from the LUMO levels and band gaps. All of compounds showed narrower energy levels in thin film state compared with solution state. This difference was caused by the expansion of intermolecular π-π stacking due to the deposition.

Please embed Table 1. here.

Furthermore, we did theoretical calculation to investigate magnesium diethynylporphyrin derivatives in depth. All calculations were carried out using density functional theory (DFT) in Gaussian09. To reduce the computational cost, 2-

ethylhexyl group on the DPP units was alternated to isobutyl group. Figure 3 represented the optimized structure of compound **2a** and Mulliken atomic charge of nitrogen atoms. The atomic charge of the nitrogens on compound **2a** was -0.723 and this value was almost the same as -0.734 in tetraethynylporphyrin **3**. It proved that diethynylporphyrin structure with the DPP units prevented the desorption of magnesium atom. This consideration means that the DPP units adequately decrease the electronegativity of nitrogens and block the protonation of that. Previously, we invented the evaluation method of relative solubility of porphyrin derivatives using DFT calculation [31]. The relative solubility was estimated by the intermolecular interaction energy between dimer. The intermolecular interaction energy was calculated using the counterpoise method [32] which corrected a basis set superposition error (BSSE) caused in supermolecule method [33]. B3LYP method was not enough to calculate the intermolecular interaction energy because the π-π interaction energy was mainly based on the dispersion force. Therefore, as a functional method, we employed B97D3 method which could consider the dispersion force [34-36]. Then, to obtain the intermolecular interaction energy, we did firstly optimization of dimer of target porphyrin derivative using B3LYP/6-31G(d) and subsequently executed single point calculation toward the optimized structure of dimer with the counterpoise method using B97D3/6-31G(d). Figure S15 showed the optimized structure of dimer of compound **2a'** and the intermolecular interaction energies were listed in Table 2. In previous report, it was found that the solubility of porphyrin derivatives was better with lower intermolecular interaction energy. As shown Table 2, diethynylporphyrin derivatives indicated small interaction energy than tetraethynylporphyrin derivative **3**. It was explained that the electron rich units directly connecting to the porphyrin core inhibited the intermolecular interaction because those units were twisted structure toward the porphyrin core. This proved diethynylporphyrin derivatives had good solubility than tetraethynyl porphyrin derivatives with long alkyl chain units. Further, we did time-dependent DFT (TD-DFT) calculation to explore photophysical property of diethynylporphyrin derivatives. Figure 4 represented the calculated UV-vis spectrum of compound **2b'**. As with the actual survey (Figure 2), the calculation showed that compound **2b'** had a maximum peak in the Q band area and the oscillator strength of Q band peak was 2.30.

Please embed Fig 3. here.

Please embed Fig 4. here.

Please embed Table 2. here.

We fabricated solution-processed bulk heterojunction OSCs using compound **2a** and **2b** as a small-molecule donor material. As an acceptor material, phenyl-C61-butyric acid methyl ester ($PC_{61}BM$) was employed. The device structure was ITO/PEDOT:PSS/**2a** or **2b**+ $PC_{61}BM$/LiF/Al (ITO = indium tin oxide; PEDOT:PSS = poly(3,4-ethylenedioxythiophene):polystyrene sulfonate). We investigated a morphology of the active layer by atomic force microscopy (AFM) (Figure 5). AFM images revealed the combination of those diethynylporphyrin derivatives and $PC_{61}BM$ caused the formation of moderate grain size. Table 3 summarizes the device performance under 100 mW/cm^2 simulated solar irradiation. We fixed the conditions as follows: (1) donor/acceptor ratio, 1:1.5; (2) thermal annealing time, 10 min; (3) solvent vapor annealing (SVA) time, 30 s; (4) concentration of donor acceptor mixture, 30 mg/mL; (5) solvent, chlorobenzene; and (6) additive, 1% pyridine. The best condition gave a PCE of 2.91% in compound **2a** and 1.20% in compound **2b** (Figure 6). Although we also applicated compound **2a** and **2b** for inverted organic solar cells, those devices gave PCE of less than 1% (Table S2).

Please embed Fig 5. here.

Please embed Fig 6. here.

Please embed Table 3. here.

CONCLUSION

We synthesized first magnesium diethynylporphyrin derivatives **2a** and **2b** with the electron rich units. Those electron rich units effected photophysical property. In compound **2b**, the maximum absorption efficient was assigned to the Q band peak. This interesting observation was derived from the intramolecular charge transfer. Not only the easies of synthesis, diethynylporphyrin structure had a merit for the solubility which was an important factor to use porphyrin derivatives as an organic semiconductor material. Therefore, we believed that magnesium diethynylporphyrin derivatives had a potential to accelerate the progress of OSCs and thought a necessity to explore this new porphyrin material.

REFERENCES

1. Zhou R, Jiang Z, Yang C, Yu J, Feng J, Adil MA, Deng D, Zou W, Zhang J, Lu K, Ma W, Gao F and Wei Z. *Nat Commun*. 2019; **10**: 5393.
2. Yadagiri B, Narayanaswamy K, Revoju S, Eliasson B, Sharma GD and Singh SP. *Journal of Materials Chemistry C*. 2019; **7**: 709-717.
3. Yang D, Wang Y, Sano T, Gao F, Sasabe H and Kido *J. Journal of Materials Chemistry A*. 2018; **6**: 13918-13924.
4. Yang L, Zhang S, He C, Zhang J, Yao H, Yang Y, Zhang Y, Zhao W and Hou J. *J. Am. Chem. Soc.* 2017; **139**: 1958-1966.
5. Qiu B, Xue L, Yang Y, Bin H, Zhang Y, Zhang C, Xiao M, Park K, Morrison W, Zhang Z-G and Li Y. *Chem. Mater.* 2017; **29**: 7543-7553.
6. Collins SD, Ran NA, Heiber MC and Nguyen T-Q. *Advanced Energy Materials* 2017; 7.
7. Deng D, Zhang Y, Yuan L, He C, Lu K and Wei Z. *Advanced Energy Materials* 2014; 4.
8. Chen S, Xiao L, Zhu X, Peng X, Wong WK and Wong WY. *Chem Commun.* 2015; **51**: 14439-14442.
9. Vijay Kumar C, Cabau L, Koukaras EN, Sharma GD and Palomares E. *Nanoscale*. 2015; **7**: 179-189.
10. Xiao L, Chen S, Gao K, Peng X, Liu F, Cao Y, Wong WY, Wong WK and Zhu X. *ACS Appl Mater Interfaces*. 2016; **8**: 30176-30183.
11. Gao K, Xiao L, Kan Y, Yang B, Peng J, Cao Y, Liu F, Russell TP and Peng X. *Journal of Materials Chemistry C*. 2016; **4**: 3843-3850.
12. Morán G, Arrechea S, Cruz Pdl, Cuesta V, Biswas S, Palomares E, Sharma GD and Langa F. *Journal of Materials Chemistry A*. 2016; **4**: 11009-11022.
13. Arrechea S, Aljarilla A, de la Cruz P, Singh MK, Sharma GD and Langa F. *Journal of Materials Chemistry C.* 2017; **5**: 4742-4751.
14. Zhang A, Li C, Yang F, Zhang J, Wang Z, Wei Z and Li W. *Angew. Chem. Int. Ed. Engl.* 2017; **56**: 2694-2698.
15. Hatano J, Obata N, Yamaguchi S, Yasuda T and Matsuo Y. *J. Mater. Chem.* 2012; **22**: 19258-19263.
16. Yamamoto T, Hatano J, Nakagawa T, Yamaguchi S and Matsuo Y. *Appl. Phys. Lett.* 2013; **102**: 013305.
17. Matsuo Y, Hatano J and Nakagawa T. *J. Phys. Org. Chem.* 2014; **27**: 87-93.

18. Sato T, Nakagawa T, Okada H and Matsuo Y. *J. Porphyrins Phthalocyanines.* 2015; **19**: 451-458.
19. Nakagawa T, Wang H, Zieleniewska A, Okada H, Aoyagi S, Guldi DM and Matsuo Y. *Chem Asian J.* 2018; **13**: 3032-3039.
20. Li L, Huang Y, Peng J, Cao Y and Peng X. *J. Mater. Chem. A*. 2013; **1**: 2144-2150.
21. Qin H, Li L, Guo F, Su S, Peng J, Cao Y and Peng X. *Energy Environ. Sci.* 2014; **7**: 1397-1401.
22. Gao K, Li L, Lai T, Xiao L, Huang Y, Huang F, Peng J, Cao Y, Liu F, Russell TP, Janssen RA and Peng X. *J. Am. Chem. Soc.* 2015; **137**: 7282-7285.
23. Li M, Gao K, Wan X, Zhang Q, Kan B, Xia R, Liu F, Yang X, Feng H, Ni W, Wang Y, Peng J, Zhang H, Liang Z, Yip H-L, Peng X, Cao Y and Chen Y. *Nature Photonics*. 2016; **11**: 85-90.
24. Lai T, Chen X, Xiao L, Zhang L, Liang T, Peng X and Cao Y. *Chem Commun*. 2017; **53**: 5113-5116.
25. Takahashi K, Kumagai D, Yamada N, Kuzuhara D, Yamaguchi Y, Aratani N, Koganezawa T, Koshika S, Yoshimoto N, Masuo S, Suzuki M, Nakayama K-i and Yamada H. *Journal of Materials Chemistry A* 2017; **5**: 14003-14011.
26. Hadmojo WT, Yim D, Sinaga S, Lee W, Ryu DY, Jang W-D, Jung IH and Jang S-Y. *ACS Sustainable Chemistry & Engineering*. 2018; **6**: 5306-5313.
27. Ogumi K, Nakagawa T, Okada H, Sakai R, Wang H and Matsuo Y. *Journal of Materials Chemistry A*. 2017; **5**: 23067-23077.
28. Wang H, Nakagawa T, Zhang M-M, Ogumi K, Yang S and Matsuo Y. *RSC Advances*. 2019; **9**: 32562-32572.
29. Wang H, Yue Q, Nakagawa T, Zieleniewska A, Okada H, Ogumi K, Ueno H, Guldi Dirk M, Zhu X and Matsuo Y. *Journal of Materials Chemistry A*. 2019; **7**: 4072-4083.
30. Ogumi K, Nakagawa T, Okada H and Matsuo Y. *Org. Electron.* 2019; **71**: 50-57.
31. Ogumi K and Matsuo Y. *J. Porphyrins Phthalocyanines*. 2019; **23**: 1144-1148.
32. Boys SF and Bernardi F. *Mol. Phys.* 1970; **19**: 553-566.
33. Ransil BJ. *J. Chem. Phys.* 1961; **132**: 154104.
34. Becke AD. *J. Chem. Phys.* 1997; **107**: 8554-8560.
35. Becke AD. *J. Chem. Phys.* 1998; **109**: 2092-2098.
36. Grimme S. J. *Comput. Chem.* 2006; *27*: 1787-1799.

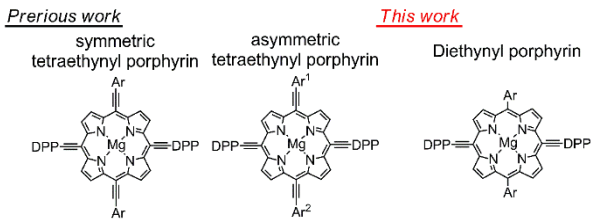

Fig. 1. Representation of magnesium diethynylporphyrin derivatives.

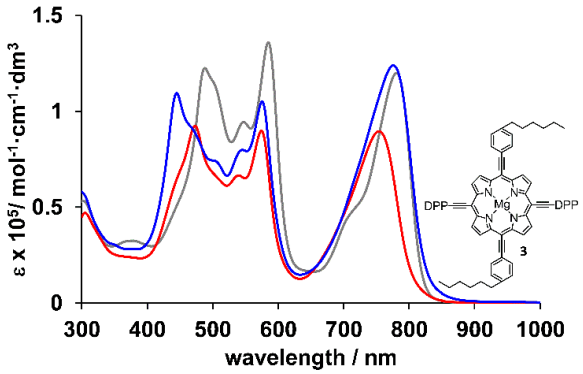

Fig. 2. UV-vis spectra of compound **2a** (red), **2b** (blue) and **3** (gray) in THF solution.

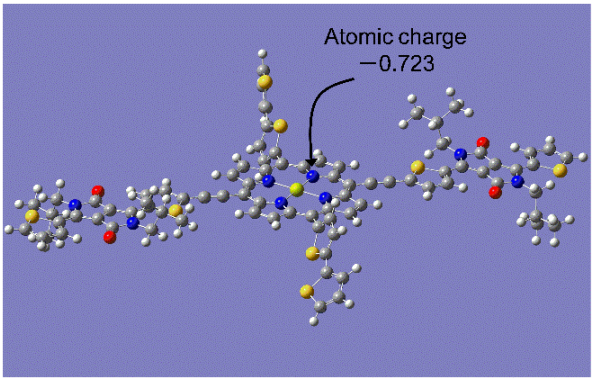

Fig. 3. Optimized structure of compound **2a'**.

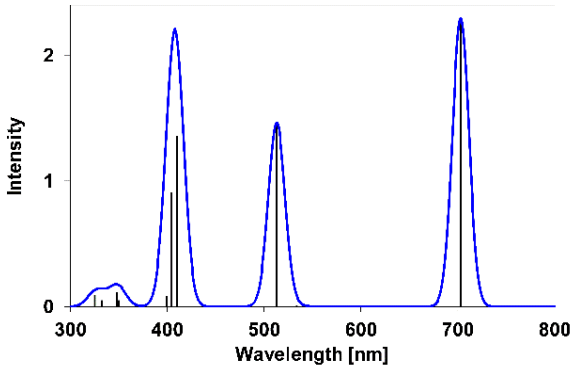

Fig. 4. Simulated UV-vis spectrum of compound **2b'**

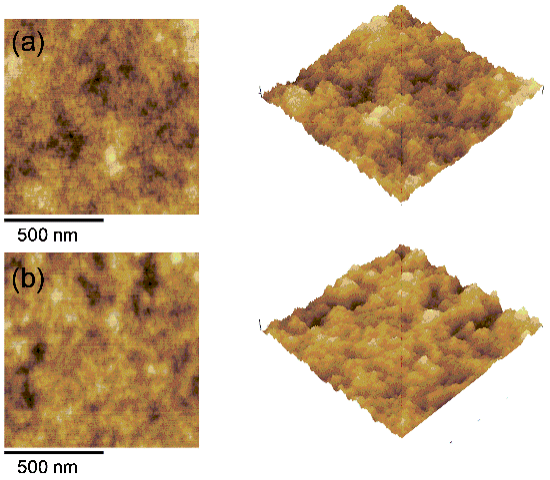

Fig. 5. AFM images of the surface of active layer (1 μm x 1 μm). (a) Compound **2a** + $PC_{61}BM$. (b) Compound **2b** + $PC_{61}BM$.

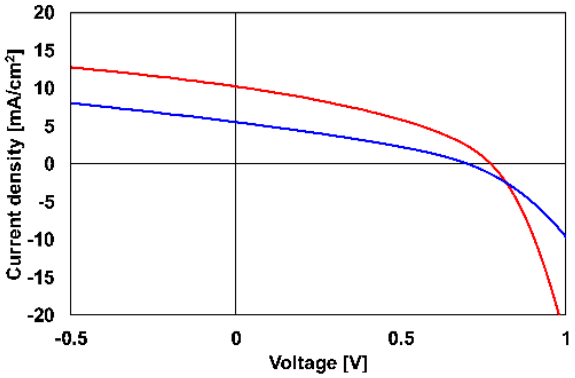

Fig. 6. J–V curves of optimized devices by using **2a** (red line), **2b** (blue line).

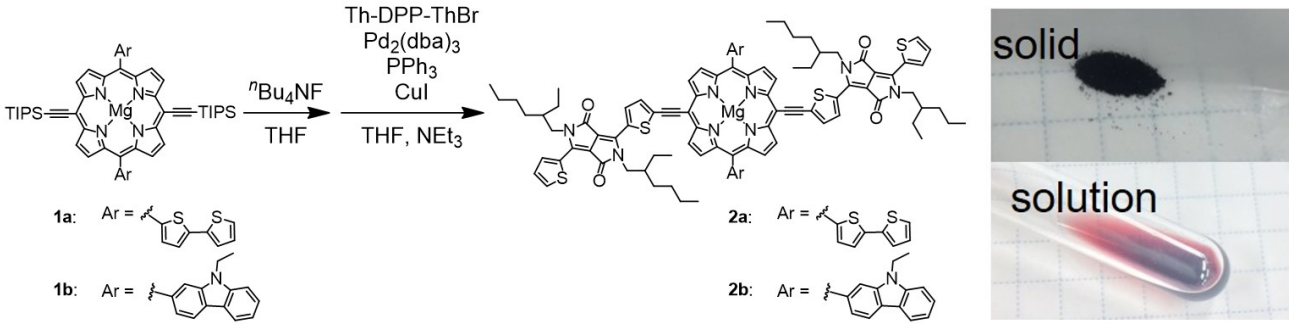

Scheme 1. Synthesis of magnesium tetraethynyl porphyrin derivatives **2a** and **2b**.

Table 1. Electrochemical properties of compound **2a**, **2b** and **3**.

Compound	Solution[a] HOMO [eV]	LUMO [eV]	E_g [eV]	Film[b] HOMO[c] [eV]	LUMO[d] [eV]	E_g[e] [eV]
2a	−4.94	−3.20	1.74	−5.11	−3.79	1.32
2b	−5.06	−3.38	1.68	−5.00	−3.73	1.27
3	−5.12	−3.43	1.69	−5.25	−3.91	1.34

[a] Values were determined by DPV. Measurements were performed in THF solution containing $TBAPF_6$ (0.1 M) as a supporting electrolyte at 25 °C at a scan rate of 100 mV s^{-1}. Glassy-carbon, platinum wire, and $Ag/AgClO_4$ electrodes were used as the working, counter, and reference electrodes, respectively. The potential was corrected against Fc/Fc^+. The HOMO and LUMO levels were estimated by using the following equations: HOMO = $-(4.8 + E^{ox}_{1/2})$, LUMO = $-(4.8 + E^{red}_{1/2})$. E_g = LUMO – HOMO. [b] Cast film. [c] HOMO levels in film were determined by PYS. [d] LUMO = HOMO + E_g. [e] HOMO–LUMO band gaps were determined by UV-vis spectroscopy in the film state.

Table 2. DFT calculation of optimized dimer of compound **2a'**, **2b'** and **3** (kcal/mol).

Compound	Energy of dimer	Intermolecular interaction energy	BSSE
2a'	−9242014.97	−25.62	−5.21
2b'	−7965118.34	−32.10	−6.04
3	−7338446.43	−44.89	−10.0

Table 3. Photovoltaic performance of devices using compound **2a** and **2b**.

donor	acceptor	TA [°C]	SVA	V_{OC} [V]	J_{SC} [mA/cm^2]	FF [%]	PCE [%]
2a	$PC_{61}BM$	80	—	0.773	10.25	36.6	2.91
2a	$PC_{61}BM$	100	—	0.772	10.24	36.2	2.86
2a	$PC_{61}BM$	120	—	0.767	8.19	33.1	2.08
2b	$PC_{61}BM$	—	—	0.703	4.919	28.2	0.97
2b	$PC_{61}BM$	—	THF	0.699	5.086	28.0	0.99
2b	$PC_{61}BM$	100	—	0.702	5.485	31.1	1.20

Magnesium diethynylporphyrin derivatives with strong near-infrared absorption for solution-process bulk heterojunction organic solar cells

Keisuke Ogumi, Takafumi Nakagawa, Masahiro Nakano and Yutaka Matsuo*

We synthesized novel magnesium diethynylporphyrin derivatives with the electron rich units. Those units influenced photophysical properties and gave the strong rear-infrared absorption due to the intramolecular charge transfer. Diethynylporphyrin structure also inproves the solubility because of the inhibition of intermolecular interaction. The optimised device using magnesium diethynyl porphyrin derivative gave a PCE of 2.91%.